Journal of Systems Engineering and Electronics
Vol. 32, No. 4, August 2021, pp.756 – 763

A search-free near-field source localization method with exact signal model

PAN Jingjing[1,2], SINGH Parth Raj[3], and MEN Shaoyang[4,*]

1. Key Laboratory of Dynamic Cognitive System of Electromagnetic Spectrum Space, Nanjing University of Aeronautics and Astronautics, Nanjing 211106, China; 2. Department of Electronic Engineering, Nanjing University of Aeronautics and Astronautics, Nanjing 211106, China; 3. International Electronics Engineering S.A., Bissen L-7795, Luxembourg; 4. School of Medical Information Engineering, Guangzhou University of Chinese Medicine, Guangzhou 510006, China

Abstract: Most of the near-field source localization methods are developed with the approximated signal model, because the phases of the received near-field signal are highly non-linear. Nevertheless, the approximated signal model based methods suffer from model mismatch and performance degradation while the exact signal model based estimation methods usually involve parameter searching or multiple decomposition procedures. In this paper, a search-free near-field source localization method is proposed with the exact signal model. Firstly, the approximative estimates of the direction of arrival (DOA) and range are obtained by using the approximated signal model based method through parameter separation and polynomial rooting operations. Then, the approximative estimates are corrected with the exact signal model according to the exact expressions of phase difference in near-field observations. The proposed method avoids spectral searching and parameter pairing and has enhanced estimation performance. Numerical simulations are provided to demonstrate the effectiveness of the proposed method.

Keywords: near-field, source localization, polynomial rooting, approximation error, exact signal model.

DOI: 10.23919/JSEE.2021.000065

1. Introduction

Source localization is of practical importance in many aspects of array signal processing, for example, radar, sonar, speech, and seismology [1−5]. When a source is located in the Fresnel region of an array, the near-field, its wave front is spherical and the phase difference among sensors is non-linear. Therefore, both direction of arrival (DOA) and the range are necessary for the localization of near-field sources.

Most of the near-field source localization methods are based on an approximated signal model for simplification [6−8]. The phase difference is usually approximated as a linear term which contains only the DOA, like in the far-field, and a quadratic non-linear term which contains both the DOA and the range. Several source localization methods aim at the elimination of the quadratic non-linear term to reduce the computational complexity, which only needs several one-dimensional (1-D) search. This type of 1-D spectral methods includes the covariance approximation method [9], the weighted linear prediction method [10], the rank reduced (RARE) method [11], the second order statistics (SOS) method [12], the reduced-dimension method [13], and the high order statistics based methods [2,14−16].

Unfortunately, the approximated model based methods suffer from model mismatch, resulting in systematic estimation bias in practical environment [17−19]. In the literature, there are two main approaches dealing with the exact signal model in near-field source localization. One is to directly estimate the DOA and the range with the exact model, including the maximum likelihood estimator (MLE) method [20], the Fourier transform method [21], the parallel factor (PARAFAC) decomposition method [22], and the cumulant based method [17]. However, direct estimation methods generally require multi-dimensional or 1-D search, or multiple decomposition, which brings much computational load. The other approach performs an initial estimate of DOA and range by using the approximated signal model based methods, followed by error correction procedures [22,23]. Although the family of the approximated model based methods [7,9−16] perform reduced-dimension estimation, they still need several 1-D search or parameter pairing operations, which

Manuscript received November 24, 2020.
*Corresponding author.
This work was supported by the Key Laboratory of Dynamic Cognitive System of Electromagnetic Spectrum Space (KF20202109), the National Natural Science Foundation of China (82004259), and the Young Talent Training Project of Guangzhou University of Chinese Medicine (QNYC20190110).

have an influence on the estimation accuracy and efficiency.

In this paper, a search-free near-field source localization method is proposed with the exact signal model by using the correction method. The contributions of this work are as follows:

(i) Reduce the computational complexity of the approximated model based near-filed source localization methods. Unlike [23], the proposed method obtains the estimates of DOA and range with the approximated signal model through parameter separation and the polynomial rooting, which is free of searching and pairing.

(ii) Improve the parameter estimation accuracy in near-field source localization. Compared with the spectral methods, rooting procedures are more effective in parameter estimation problems [24]. Besides, the implementation of error correction also contributes to the reduction of systematic estimation error with the approximated signal model.

The rest of this paper is organized as follows. Section 2 presents the signal model. Section 3 describes the proposed method. Section 4 gives the theoretical analysis. Section 5 shows its performance with numerical data. Conclusions are drawn in Section 6.

2. Signal model

Consider K independent narrow band signals impinging on a uniform linear array (ULA) with elements, as shown in Fig. 1.

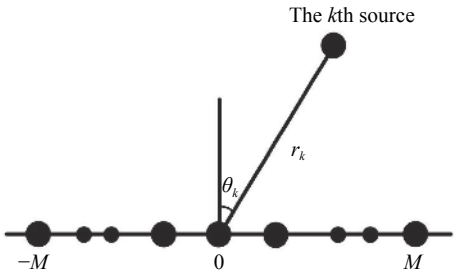

Fig. 1 ULA configuration in near-field source localization

Taking the 0th element as reference, the received signal at the mth sensor can be expressed as

$$x_m(t)=\sum_{k=1}^{K}s_k(t)\mathrm{e}^{\mathrm{j}\delta_{mk}}+n_m(t) \tag{1}$$

where $n_m(t)$ is the additive white Gaussian noise at the mth sensor with zero mean and variance σ^2; $s_k(t)$ is the signal emitted from the kth source and received by the mth sensor at time t, $t\in[1,L]$; L denotes the number of snapshots; δ_{mk} denotes the phase difference of the kth signal between sensors m and 0:

$$\delta_{mk}=\frac{2\pi}{\lambda}\left(\sqrt{r_k^2+(md)^2-2md\sin\theta_k}-r_k\right) \tag{2}$$

where θ_k denotes the DOA of the kth source, $\theta_k\in\left[-\frac{\pi}{2},\frac{\pi}{2}\right]$; r_k is the range of the kth source, which is within the Fresnel region $r_F\in[0.62(D^3/\lambda)^{1/2},2D^2/\lambda]$; D is the array aperture; λ is the wavelength of incoming signals; and d denotes the distance between two adjacent elements of ULA.

The phase difference in (2) is usually approximated by using the second-order Taylor expansion [25,26]:

$$\delta_{mk}\approx\left(-\frac{2\pi d}{\lambda}\sin\theta_k\right)m+\left(\frac{\pi d^2}{\lambda r_k}\cos^2\theta_k\right)m^2\approx\omega_k m+\phi_k m^2 \tag{3}$$

with $\omega_k=-\frac{2\pi d}{\lambda}\sin\theta_k$ and $\phi_k=\frac{\pi d^2}{\lambda r_k}\cos^2\theta_k$.

The vector of the received signal can be written as

$$\boldsymbol{x}(t)=\boldsymbol{A}\boldsymbol{s}(t)+\boldsymbol{n}(t) \tag{4}$$

where $\boldsymbol{x}(t)=[x_{-M}(t),x_{-M+1}(t),\cdots,x_M(t)]^{\mathrm{T}}$, $\boldsymbol{s}(t)=[s_1(t),s_2(t),\cdots,s_K(t)]^{\mathrm{T}}$ $\boldsymbol{n}(t)=[n_{-M}(t),n_{-M+1}(t),\cdots,n_M(t)]^{\mathrm{T}}$, $\boldsymbol{A}=[\boldsymbol{a}(r_1,\theta_1),\boldsymbol{a}(r_2,\theta_2),\cdots,\boldsymbol{a}(r_K,\theta_K)]$ is the steering matrix; $\boldsymbol{a}(r_k,\theta_k)=[\mathrm{e}^{\mathrm{j}\delta_{-Mk}},\cdots,\mathrm{e}^{\mathrm{j}\delta_{Mk}}]^{\mathrm{T}}$, where δ_{-Mk} can either be the exact or the approximated phase differences.

The covariance matrix of the received signals is

$$\boldsymbol{R}=\mathrm{E}\left[\boldsymbol{x}(t)\boldsymbol{x}^{\mathrm{H}}(t)\right]=\boldsymbol{A}\boldsymbol{R}_s\boldsymbol{A}^{\mathrm{H}}+\sigma^2\boldsymbol{I} \tag{5}$$

where $\boldsymbol{R}_s=\mathrm{E}\left[\boldsymbol{s}(t)\boldsymbol{s}^{\mathrm{H}}(t)\right]$ is the covariance matrix of the source signals, $\mathrm{E}[\cdot]$ denotes the ensemble average, and $\boldsymbol{I}$ is the identity matrix.

The eigenvalue decomposition (EVD) of $\boldsymbol{R}$ is

$$\boldsymbol{R}=\boldsymbol{U}\boldsymbol{\Lambda}\boldsymbol{U}^{\mathrm{H}} \tag{6}$$

where $\boldsymbol{\Lambda}$ is a diagonal matrix whose elements are the eigenvalues of $\boldsymbol{R}$ in descending order, $\lambda_1\geqslant\cdots\geqslant\lambda_K>\lambda_{K+1}=\cdots=\lambda_N=\sigma^2$ and $\boldsymbol{U}=[\boldsymbol{u}_1,\boldsymbol{u}_2,\cdots,\boldsymbol{u}_N]$ contains the corresponding eigenvectors.

3. Methodology

For the source localization with the exact signal model, we propose to firstly apply an approximated signal model based method to obtain the initial approximative estimates of DOA and range, and then perform error correction with respect to the exact phase difference and signal model. The approximated estimation of DOA and range is achieved by the polynomial rooting procedure with the approximated signal model.

3.1 Polynomial rooting with approximated signal model

In approximated signal model based methods, the steer-

ing vector can be represented by using parameter separation in the following split form [13]:

$$\boldsymbol{a}(r,\theta)=\underbrace{\begin{bmatrix} \mathrm{e}^{\mathrm{j}(-M)\omega} & & & & \\ & \mathrm{e}^{\mathrm{j}(-M+1)\omega} & & & \\ & & \ddots & & \\ & & & 1 & \\ & & & & \mathrm{e}^{\mathrm{j}(M-1)\omega} \\ & & & & \mathrm{e}^{\mathrm{j}M\omega} \end{bmatrix}}_{\boldsymbol{\Gamma}(\omega)} \underbrace{\begin{bmatrix} \mathrm{e}^{\mathrm{j}M^2\phi} \\ \mathrm{e}^{\mathrm{j}(M-1)^2\phi} \\ \vdots \\ 1 \end{bmatrix}}_{\boldsymbol{b}(\phi)} \tag{7}$$

where $\boldsymbol{\Gamma}(\omega)$ only contains the information of DOA while $\boldsymbol{b}(\phi)$ contains both the information of DOA and range.

With the split of DOA and range, the searching spectrum of multiple signal classification (MUSIC) with the approximated signal model becomes

$$P_{\mathrm{MUSIC}}(r,\theta)=\min_{r,\theta}\boldsymbol{a}^{\mathrm{H}}(r,\theta)\boldsymbol{U}_n\boldsymbol{U}_n^{\mathrm{H}}\boldsymbol{a}(r,\theta)=$$
$$\min_{\omega,\phi}\boldsymbol{b}^{\mathrm{H}}(\phi)\underbrace{\boldsymbol{\Gamma}^{\mathrm{H}}(\omega)\boldsymbol{U}_n\boldsymbol{U}_n^{\mathrm{H}}\boldsymbol{\Gamma}(\omega)}_{\boldsymbol{Q}(\omega)}\boldsymbol{b}(\phi) \tag{8}$$

where $\boldsymbol{U}_n=[\boldsymbol{u}_{K+1},\boldsymbol{u}_{K+2},\cdots,\boldsymbol{u}_N]$.

According to the Rayleigh quotient theorem [27], the minimum of the quadratic function in (8) over ω and ϕ is equal to the minimum eigenvalue of $\boldsymbol{Q}(\omega)$. Since $\boldsymbol{Q}(\omega)$ is with the quadratic form, its eigenvalues are always non-negative [28]. When ω corresponds to the true DOA of a near-field source, the minimum eigenvalue is equal to zero and the determinant of $\boldsymbol{Q}(\omega)$ reaches zero as well.

Assume $z=\mathrm{e}^{-\mathrm{j}\frac{2\pi d}{\lambda}\sin\theta}$, $\boldsymbol{\Gamma}(\omega)$ can be represented as

$$\boldsymbol{\Gamma}(\omega)=\boldsymbol{\Gamma}(z)=\begin{bmatrix} z^{(-M)} & & & & \\ & z^{(-M+1)} & & & \\ & & \ddots & & \\ & & & 1 & \\ & & & & z^{(M-1)} \\ & & & & z^{(M)} \end{bmatrix}. \tag{9}$$

Therefore, the angle information of the near-field sources can be obtained by finding the values of z satisfying

$$\det[\boldsymbol{Q}(\omega)]=\det\left[\boldsymbol{\Gamma}^{\mathrm{T}}\left(z^{-1}\right)\boldsymbol{U}_n\boldsymbol{U}_n^{\mathrm{H}}\boldsymbol{\Gamma}(z)\right] \tag{10}$$

where $\det[\cdot]$ denotes the determinant.

Since $\boldsymbol{\Gamma}(\omega)$ is a symmetric matrix, it is easy to find that the expression of $\det[\boldsymbol{Q}(\omega)]$ is an even function. According to the basic property of the even function, (10) can be represented as the following polynomial:

$$f(z)=\gamma_1\prod_{n=1}^{\frac{M(M+1)}{2}}(1-z_nz^{-1})(1-z_n^*z)(1+z_nz^{-1})(1+z_n^*z) \tag{11}$$

where γ_1 is a constant.

In theory, the roots of (11) are not only conjugate reciprocal but also rotational symmetric with respect to the origin. Therefore, there will be $2K$ roots lying inside and close to the unit circle. However, the phase of $z=\mathrm{e}^{-\mathrm{j}\frac{2\pi d}{\lambda}\sin\theta}$ is limited to $\left[-\frac{\pi}{2},\frac{\pi}{2}\right]$ since $d\leqslant\frac{\lambda}{4}$ in the approximated signal model based methods. In this context, the K roots corresponding to the true DOAs can be selected for the estimation

$$\widetilde{\theta}_k=-\arcsin\left(\angle z_k\frac{\lambda}{2\pi d}\right) \tag{12}$$

where $\angle$ represents the phase of a complex variable.

Substituting each estimated DOA into (8), we can formulate another polynomial:

$$\boldsymbol{b}^{\mathrm{T}}\left(v^{-1}\right)\boldsymbol{Q}(\widetilde{\omega}_k)\boldsymbol{b}(v)=0 \tag{13}$$

where $v=\mathrm{e}^{-\mathrm{j}\frac{\pi d^2}{\lambda r}\cos^2\widetilde{\theta}_k}$. Similarly, (13) can be represented as

$$g(z)=\gamma_2\prod_{n=1}^{(M+1)^2}(1-v_nv^{-1})(1-v_n^*v) \tag{14}$$

where γ_2 is a constant.

With the approximative estimate $\widetilde{\theta}_k$, there is only one root lying inside and close to the unit circle, v_k, which can be used for the range estimation:

$$\widetilde{r}_k=\frac{\pi d^2}{\lambda\angle v_k}\cos^2\widetilde{\theta}_k. \tag{15}$$

It should be noted that the proposed method is search-free and computational efficient. The range parameter is calculated with each estimated DOA, which does not require an additional pairing procedure.

3.2 Error correction with exact signal model

Let $(\widetilde{r}_k,\widetilde{\theta}_k)$ be the initial estimates of DOA and range of the kth source with the approximated signal model. The approximated phase difference is

$$\widetilde{\delta}_{mk}=\left(-\frac{2\pi d}{\lambda}\sin\widetilde{\theta}_k\right)m+\left(\frac{\pi d^2}{\lambda\widetilde{r}_k}\cos^2\widetilde{\theta}_k\right)m^2. \tag{16}$$

As mentioned in [23], the parameters can be corrected with the approximative estimates by using (2):

$$2\widetilde{\delta}_{mk}\frac{\lambda}{2\pi}r_k+2mdr_k\sin\theta_k=(md)^2-\left(\widetilde{\delta}_{mk}\frac{\lambda}{2\pi}\right)^2. \tag{17}$$

Since $m\in[-M,M]$, we can form the following system of linear equations for the kth source:

$$\underbrace{\begin{bmatrix} 2\tilde{\delta}_{-Mk}\dfrac{\lambda}{2\pi} & 2(-M)d \\ \vdots & \vdots \\ 2\tilde{\delta}_{0k}\dfrac{\lambda}{2\pi} & 0 \\ \vdots & \vdots \\ 2\tilde{\delta}_{Mk}\dfrac{\lambda}{2\pi} & 2(M)d \end{bmatrix}}_{\boldsymbol{D}} \begin{bmatrix} r_k \\ r_k\sin\theta_k \end{bmatrix} = \underbrace{\begin{bmatrix} (-Md)^2-\left(\tilde{\delta}_{-Mk}\dfrac{\lambda}{2\pi}\right)^2 \\ \vdots \\ 0-\left(\tilde{\delta}_{0k}\dfrac{\lambda}{2\pi}\right)^2 \\ \vdots \\ (Md)^2-\left(\tilde{\delta}_{Mk}\dfrac{\lambda}{2\pi}\right)^2 \end{bmatrix}}_{\boldsymbol{c}}. \tag{18}$$

Finally, the corrected estimates of each source can be obtained by

$$\begin{cases} \widehat{r_k} = \Psi(1) \\ \widehat{\theta_k} = \sin^{-1}\left(\dfrac{\Psi(2)}{\Psi(1)}\right) \end{cases} \tag{19}$$

where $\boldsymbol{\Psi} = \boldsymbol{D}^{+}\boldsymbol{c}$.

The proposed method is summarized as follows:

(i) Estimate the data covariance matrix $\boldsymbol{R}$ and apply EVD on it;

(ii) Build polynomials (11), (14) and obtain the approximated DOA and range;

(iii) Calculate $\widetilde{\delta}_{mk}$ for each source by using the approximative estimates;

(iv) Construct the linear system of equations for each source and obtain the corrected estimates of DOA and range.

The computational complexity of the proposed method is $O\{N^2L+N^3+(N^2-1)/4+K((N^2-1)/4+N^3+N)\}$, while that of [23] is $O\{N^2L+N^3+Kn_\theta(N-K)(N+1)+n_r(N-K)(N+1)(3N+1)/4+K(N^3+N)\}$, where n_θ and n_r denote the searching number in the DOA and the range domain, respectively.

4. Theoretical analysis

4.1 Asymptotic properties of the rooting procedure with approximated signal model

The asymptotic performance of the proposed method is analyzed with a sufficiently large number of snapshots. In the presence of noise, the errors in the eigenvectors lead to the perturbations in the signal zeros, both in the estimation of DOA and range. Here, we only show the estimation error of the rooting procedure with the approximated signal model.

Let z_k and v_k be the signal zero in the estimation of DOA and range for the source respectively, that is, $|z_k|=1$ and $|v_k|=1$. Assume Δz_k and Δv_k as the estimation error. Therefore, the mean square error of the signal zeros $\overline{|\Delta z_k|^2}$ and $\overline{|\Delta v_k|^2}$ can be given as follows.

Firstly, for the determination of $\overline{|\Delta z_k|^2}$, the polynomial (11) with estimation errors can be expressed as

$$\begin{aligned} \tilde{f}(z_k) &= \gamma_1 \prod_{n=1}^{\frac{M(M+1)}{2}} \left(1-(z_n+\Delta z_n)z^{-1}\right)(1-(z_n+\Delta z_n)^{*}z)(1+ \\ &\quad (z_n+\Delta z_n)z^{-1})(1+(z_n+\Delta z_n)^{*}z) = \\ &\tilde{\gamma}_1|\Delta z_k|^4 \prod_{n=1,n=k}^{\frac{M(M+1)}{2}} \left|1-(z_n+\Delta z_n)z_k^{-1}\right|^2\left|1+(z_n+\Delta z_n)z_k^{-1}\right|^2 \approx \\ &\quad \tilde{\gamma}_1|\Delta z_k|^4 \prod_{n=1,n=k}^{\frac{M(M+1)}{2}} |(1-z_nz_k^{-1})|^2|1+z_nz_k^{-1}|^2 \end{aligned} \tag{20}$$

with higher order terms neglected.

Taking expectations of (20), we have

$$\overline{|\Delta z_k|^2} = \sqrt{\frac{\overline{\tilde{f}(z_k)}}{\tilde{\gamma}_1|\Delta z_k|^4 \prod_{n=1,n=k}^{\frac{M(M+1)}{2}} |(1-z_nz_k^{-1})|^2|1+z_nz_k^{-1}|^2}}. \tag{21}$$

According to the L' Hospital's rule and the general rules of the derivative of a determinant [29], part of the expression in (21) can be written as

$$\frac{1}{\prod_{n=1,n=k}^{\frac{M(M+1)}{2}}\left|1-z_nz_k^{-1}\right|^2\left|1+z_nz_k^{-1}\right|^2} = \lim_{z\to z_k}\frac{\left|1-z_nz_k^{-1}\right|^2\left|1+z_nz_k^{-1}\right|^2}{f(z)} = \lim_{\omega\to\omega_k}\frac{\left|1-\mathrm{e}^{\mathrm{j}(\omega_k-\omega)}\right|^2\left|1+\mathrm{e}^{\mathrm{j}(\omega_k-\omega)}\right|^2}{\det[\boldsymbol{Q}(\omega)]} = \frac{1}{\det[\boldsymbol{Q}(\omega_k)]\,\mathrm{tr}[\boldsymbol{Q}^{-1}(\omega_k)(\boldsymbol{\Gamma}'^{\mathrm{H}}(\omega_k)\boldsymbol{U}_n\boldsymbol{U}_n^{\mathrm{H}}\boldsymbol{\Gamma}(\omega_k)+\boldsymbol{\Gamma}^{\mathrm{H}}(\omega_k)\boldsymbol{U}_n\boldsymbol{U}_n^{\mathrm{H}}\boldsymbol{\Gamma}'(\omega_k))]} \tag{22}$$

where $\boldsymbol{\Gamma}'(\omega_k)$ denotes the derivative of $\boldsymbol{\Gamma}(\omega_k)$.

Let $\boldsymbol{\eta}_k$ be the bias of the kth eigenvector $\boldsymbol{u}_k$. The expression of $\widetilde{f}(z_k)$ can be written as

$$\widetilde{f}(z_k) = \det[\boldsymbol{I}-\boldsymbol{\Gamma}^{\mathrm{H}}(\omega_k)\sum_{k=1}^{K}(\boldsymbol{u}_k+\boldsymbol{\eta}_k)(\boldsymbol{u}_k+\boldsymbol{\eta}_k)^{\mathrm{H}}\boldsymbol{\Gamma}(\omega_k)]. \tag{23}$$

As in [19], the eigenvectors and eigenvalues of $\boldsymbol{R}$ in a complex Gaussian process have the following properties:

$$\mathrm{E}(\boldsymbol{\eta}_k) = -\frac{\lambda_k}{2L}\sum_{n=1,l\neq k}^{N}\frac{\lambda_k}{(\lambda_k-\lambda_n)^2}\boldsymbol{u}_k \tag{24}$$

and

$$\mathrm{E}\left(\boldsymbol{\eta}_k\boldsymbol{\eta}_j^{\mathrm{H}}\right) = \frac{\lambda_k}{L}\sum_{n=1,l\neq k}^{N}\frac{\lambda_k}{(\lambda_k-\lambda_n)^2}\boldsymbol{u}_n\boldsymbol{u}_n^{\mathrm{H}}\xi_{kj} \tag{25}$$

where ξ_{kj} denotes the Kronecker delta.

Substituting the above expressions into (23) and then doing some mathematical operations yield [16]:

$$\overline{\widetilde{f}(z_k)} = \det\left[\frac{(N-K)\sigma^2}{L}\boldsymbol{\Gamma}^{\mathrm{H}}(\omega_k)\left(\sum_{l=1}^{K}\frac{\lambda_l}{(\lambda_l-\sigma)^2}\boldsymbol{u}_l\boldsymbol{u}_l^{\mathrm{H}}\right)\boldsymbol{\Gamma}(\omega_k)\right]. \tag{26}$$

Through the calculations, we have the expression of $\overline{|\Delta z_k|^2}$ as follows:

$$\overline{|\Delta z_k|^2} = \sqrt{\frac{\det\left[\frac{(N-K)\sigma^2}{L}\boldsymbol{\Gamma}^{\mathrm{H}}(\omega_k)\left(\sum_{l=1}^{K}\frac{\lambda_l}{(\lambda_l-\sigma)^2}\boldsymbol{u}_l\boldsymbol{u}_l^{\mathrm{H}}\right)\boldsymbol{\Gamma}(\omega_k)\right]}{\det[\boldsymbol{Q}(\omega_k)]\,\mathrm{tr}[\boldsymbol{Q}^{-1}(\omega_k)(\boldsymbol{\Gamma}'^{\mathrm{H}}(\omega_k)\boldsymbol{U}_n\boldsymbol{U}_n^{\mathrm{H}}\boldsymbol{\Gamma}(\omega_k)+\boldsymbol{\Gamma}^{\mathrm{H}}(\omega_k)\boldsymbol{U}_n\boldsymbol{U}_n^{\mathrm{H}}\boldsymbol{\Gamma}'(\omega_k))]}}. \tag{27}$$

Secondly, for the mean square error $\overline{|\Delta v_k|^2}$, we have similar derivations by using polynomial (15):

$$\widetilde{g}(v_k) = \widetilde{\gamma}_2\prod_{n=1}^{(M+1)^2}\left(1-(v_n+\Delta v_n)v_k^{-1}\right)(1-(v_n+\Delta v_n)^*v_k) \approx \widetilde{\gamma}_2|\Delta v_k|^2\prod_{n=1,n\neq k}^{(M+1)^2}|(1-v_nv_k^{-1})|^2. \tag{28}$$

Taking expectations of (28), we have

$$\overline{|\Delta v_k|^2} = \frac{\overline{\widetilde{g}(v_k)}}{\widetilde{\gamma}_2\prod_{n=1,n\neq k}^{(M+1)^2}|(1-v_nv_k^{-1})|^2} \tag{29}$$

which can be partially represented as follows:

$$\frac{1}{\widetilde{\gamma}_2\prod_{n=1,n\neq k}^{(M+1)^2}\left|1-v_nv_k^{-1}\right|^2} = \lim_{\phi\to\phi_k}\frac{\left|1-\mathrm{e}^{\mathrm{j}(\phi_k-\phi)}\right|^2}{\boldsymbol{b}^{\mathrm{H}}(\phi)\boldsymbol{Q}(\widetilde{\omega}_k)\boldsymbol{b}(\phi)} = \frac{1}{2\mathcal{R}(\boldsymbol{b}^{\mathrm{H}}(\phi_k)\boldsymbol{Q}(\widetilde{\omega}_k)\boldsymbol{b}'(\phi_k))} \tag{30}$$

where $\mathcal{R}(\cdot)$ denotes the real part and $\boldsymbol{b}'(\phi_k)$ denotes the derivative of $\boldsymbol{b}(\phi_k)$ and

$$\overline{\widetilde{g}(v_k)} = \frac{(N-K)\sigma^2}{L}\boldsymbol{b}^{\mathrm{H}}(\phi_k)\boldsymbol{\Gamma}^{\mathrm{H}}(\omega_k)\left(\sum_{l=1}^{K}\frac{\lambda_l}{(\lambda_l-\sigma)^2}\boldsymbol{u}_l\boldsymbol{u}_l^{\mathrm{H}}\right)\boldsymbol{\Gamma}(\omega_k)\boldsymbol{b}(\phi_k). \tag{31}$$

Therefore, we have the final expression of $\overline{|\Delta v_k|^2}$:

$$\overline{|\Delta v_k|^2} = \frac{\frac{(N-K)\sigma^2}{L}\boldsymbol{b}^{\mathrm{H}}(\phi_k)\boldsymbol{\Gamma}^{\mathrm{H}}(\omega_k)\left(\sum_{l=1}^{K}\frac{\lambda_l}{(\lambda_l-\sigma)^2}\boldsymbol{u}_l\boldsymbol{u}_l^{\mathrm{H}}\right)\boldsymbol{\Gamma}(\omega_k)\boldsymbol{b}(\phi_k)}{2\mathcal{R}(\boldsymbol{b}^{\mathrm{H}}(\phi_k)\boldsymbol{Q}(\widetilde{\omega}_k)\boldsymbol{b}'(\phi_k))}. \tag{32}$$

4.2 Cramer-Rao lower bound (CRLB)

The closed-form expression of the CRLB in near-field with the exact signal model is similar to that in [30]:

$$\mathrm{CRLB} = \frac{\sigma^2}{2L}\left\{\mathcal{R}\left(\left(\boldsymbol{F}^{\mathrm{H}}\prod_{\boldsymbol{A}}^{\perp}\boldsymbol{F}\right)\odot\left(\boldsymbol{1}_{2\times2}\otimes(\boldsymbol{R}_s\boldsymbol{A}^{\mathrm{H}}\boldsymbol{R}^{-1}\boldsymbol{A}\boldsymbol{R}_s)^{\mathrm{T}}\right)\right)\right\}^{-1} \tag{33}$$

where

$$\boldsymbol{1}_{2\times2} = \begin{bmatrix}1 & 1\\ 1 & 1\end{bmatrix},$$

$$\boldsymbol{F} = [\boldsymbol{f}_\theta(r_1,\theta_1),\cdots,\boldsymbol{f}_\theta(r_K,\theta_K),\boldsymbol{f}_r(r_1,\theta_1),\cdots,\boldsymbol{f}_r(r_K,\theta_K)],$$

$$\boldsymbol{f}_\theta(r_k,\theta_k) = \frac{\partial\boldsymbol{a}(r_k,\theta_k)}{\partial\theta},$$

$$\boldsymbol{f}_r(r_k,\theta_k) = \frac{\partial\boldsymbol{a}(r_k,\theta_k)}{\partial r}.$$

The derivations of $\boldsymbol{f}_\theta(r_k,\theta_k)$ and $\boldsymbol{f}_r(r_k,\theta_k)$ are realized with the exact signal model (2), without approximation.

5. Simulation

In this section, several numerical examples are presented to evaluate the performance of the proposed method. Consider a ULA with nine isotropic sensors, $M=4$. The interval between two adjacent sensors is set as $d=\frac{\lambda}{4}$. Therefore, the Fresnel region is $r_F\in[1.75\lambda,8\lambda]$. Assume two sources locate at $(4.0\lambda,-20^\circ)$ and $(6.0\lambda,20^\circ)$, respectively.

In the first simulation, the number of snapshots is $L=500$, and SNR =15 dB. Fig. 2 and Fig. 3 show the roots lying inside and close to the unit circle, in the approximated parameter estimation. In the estimation of DOA, the roots are symmetrically distributed because of the even polynomial. The roots corresponding to the

DOAs of the sources can be selected according to the phase range $\left[-\frac{\pi}{2},\frac{\pi}{2}\right]$. With the approximated estimation of DOA, we can get the approximated range of each source, see Fig. 3. Table 1 gives the estimation results of the proposed method before and after correction. It is clear that the estimations after correction are closer to the true values.

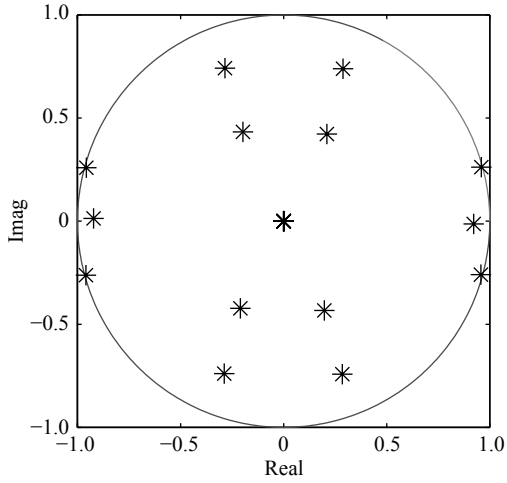

Fig. 2 Roots in the approximated estimation of DOA

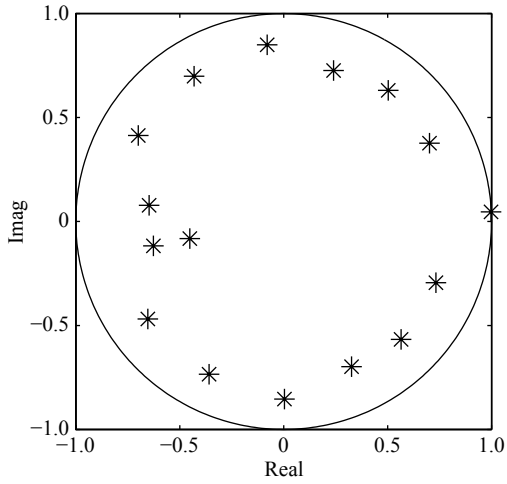

Fig. 3 Roots in the approximated estimation of range, the first source

Table 1 Near-field source localization by using the proposed method

Parameter	$\theta_1/(°)$	r_1/λ	$\theta_2/(°)$	r_2/λ
True value	−20	4	20	6
Before correction	−19.59	4.04	19.81	6.08
After correction	−19.99	3.99	20.01	6.05

In the second simulation, we analyze the statistical estimation performance of the proposed method in terms of SNR. For comparison, the estimation results of the searching method in [23] are also recorded, in which the searching step is 0.001. SNR varies from 0 to 30 dB. The other settings are the same as the first simulation. The root mean square error (RMSE) is defined as

$$\mathrm{RMSE}=\sqrt{\frac{1}{KU}\sum_{k=1}^{K}\sum_{u=1}^{U}(\widehat{\alpha}_{ku}-\alpha_k)^2} \tag{34}$$

where $\widehat{\alpha}_{ku}$ is the estimate of α_k at the uth trial, α can be DOA or range, and U is the total number of Monte Carlo trials.

Fig. 4 and Fig. 5 illustrate the RMSEs of the proposed method and that in [23] at different SNRs, before and after correction. The number of Monte Carlo trials is 200. It is obvious from the figures that the RMSEs of both methods are decreasing with the increasing of SNR, not only for the estimation of DOA but also for range. The estimations after correction are less biased, compared with those before correction. The proposed method after correction has the lowest estimation error.

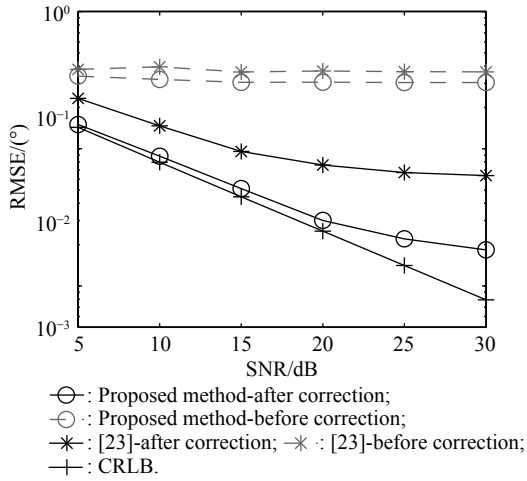

Fig. 4 RMSE in the estimation of DOA versus SNR

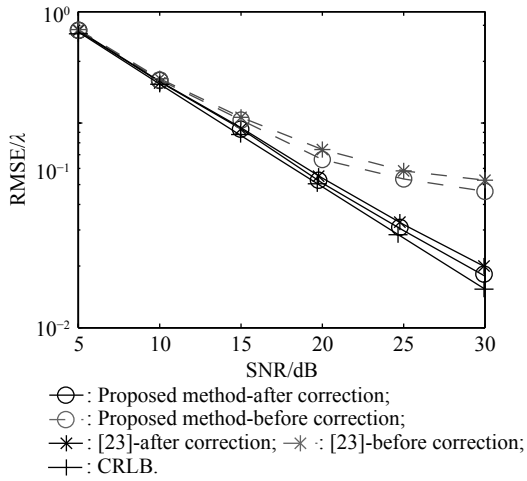

Fig. 5 RMSE in the estimation of range versus SNR

In the third simulation, we evaluate the statistical estimation performance of the proposed method with respect to the number of snapshots with 200 Monte Carlo trials, as shown in Fig. 6 and Fig. 7. The other settings are the same as the first simulation while SNR = 15 dB and the number of snapshots is within [100, 1 000]. The RMSEs of the proposed method decrease as the number of snapshots increases, like in Fig. 4 and Fig. 5. The proposed method after correction outperforms the other methods at each number of snapshots, especially for the estimation of DOA.

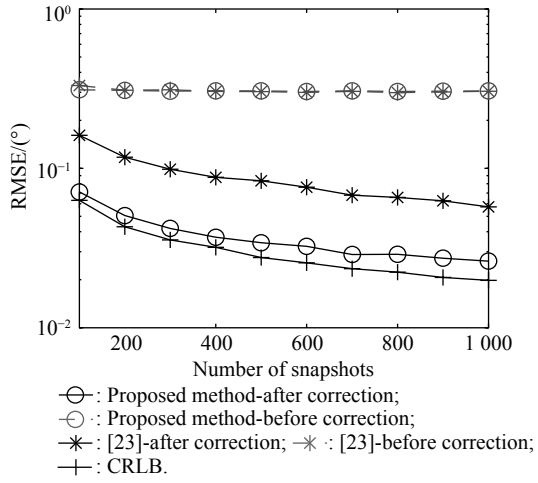

Fig. 6 RMSE in the estimation of DOA versus the number of snapshots

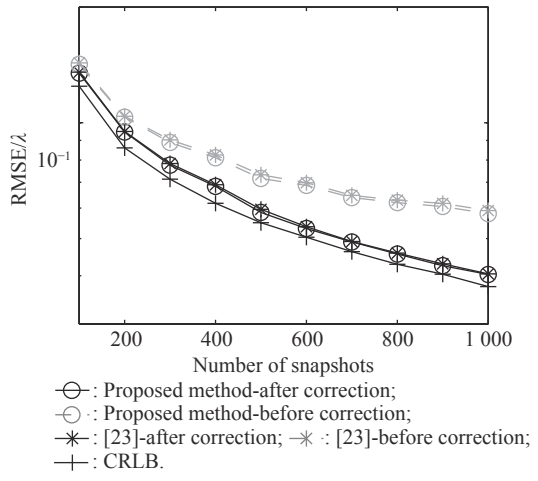

Fig. 7 RMSE in the estimation of range versus the number of snapshots

In the fourth simulation, the execution time is recorded over 200 Monte Carlo trials with L=500 and SNR = 15 dB, apart from the theoretical analysis of the complexity. The average execution time of one trail using the proposed method and that in [23] are 0.072 4 s and 0.587 4 s, respectively, with a computer equipped with a CPU of 2.2 GHz and 8 GB of RAM. In view of the execution operation time, the proposed method is much more effective compared with that in [23], since it is developed with polynomial rooting procedures.

6. Conclusions

In this paper, we propose to locate near-field sources with the exact signal model by using a search-free method. The proposed method firstly exploits the parameter separation procedure by splitting the steering vector with the approximated signal model. Then, the principle of polynomial rooting is adapted to the approximated estimation of DOA and range. The final estimates of the parameters are corrected according to the expression of the exact signal model. The proposed method requires neither searching nor pairing, which reduces the computational complexity. In addition, the estimation accuracy is improved thanks to the polynomial rooting and error correction operations. Its effectiveness is validated with the numerical simulation.

References

[1] ZUO W L, XIN J M, ZHENG N N, et al. Subspace-based near-field source localization in unknown spatially nonuniform noise environment. IEEE Trans. on Signal Processing, 2020, 68: 4713–4726.

[2] CHEN G H, ZENG X P, JIAO S, et al. High accuracy near-field localization algorithm at low SNR using fourth-order cumulant. IEEE Communications Letters, 2020, 24(3): 553–557.

[3] FRIEDLANDER B. Localization of signals in the near-field of an antenna array. IEEE Trans. on Signal Processing, 2019, 67(15): 3885–3893.

[4] LI J Z, WANG Y D, REN Z G, et al. DOA and range estimation using a uniform linear antenna array without a priori knowledge of the source number. IEEE Trans. on Antennas and Propagation, 2020, 69(5): 2929–2939.

[5] SHU T, LI L N, HE J. Near-field source localization with two-level nested arrays. IEEE Communications Letters, 2020, 24(11): 2488–2492.

[6] ZHANG X F, LI J F, XU D Z. Array signal processing and MATLAB implementation. Beijing: Publishing House of Electronics Industry, 2020. (in Chinese)

[7] ZUO W L, XIN J M, LIU W Y, et al. Localization of near-field sources based on linear prediction and oblique projection operator. IEEE Trans. on Signal Processing, 2019, 67(2): 415–430.

[8] ZUO W L, XIN J M, OHMORI H, et al. Subspace-based algorithms for localization and tracking of multiple near-field sources. IEEE Journal of Selected Topics in Signal Processing, 2019, 13(1): 156–171.

[9] LEE J H, CHEN Y M, YEH C C. A covariance approximation method for near-field direction-finding using a uniform linear array. IEEE Trans. on Signal Processing, 1995, 43(5): 1293–1298.

[10] GROSICKI E, ABED-MERAIM K, HUA Y B. A weighted linear prediction method for near-field source localization. IEEE Trans. on Signal Processing, 2005, 53(10): 3651–3660.

[11] ZHI W J, CHIA M Y W. Near-field source localization via symmetric subarrays. IEEE Signal Processing Letters, 2007, 14(6): 409–412.
[12] HE J, SWAMY M N S, AHMAD M O. Efficient application of MUSIC algorithm under the coexistence of far-field and near-field sources. IEEE Trans. on Signal Processing, 2012, 60(4): 2066–2070.
[13] ZHANG X F, CHEN W Y, ZHENG W, et al. Localization of near-field sources: a reduced-dimension MUSIC algorithm. IEEE Communications Letters, 2018, 22(7): 1422–1425.
[14] ZHENG Z, FU M C, WANG W Q, et al. Mixed far-field and near-field source localization based on subarray cross-cumulant. Signal Processing, 2018, 150: 51–56.
[15] WANG K, WANG L, SHANG J R, et al. Mixed near-field and far-field source localization based on uniform linear array partition. IEEE Sensors Journal, 2016, 16(22): 8083–8090.
[16] LIANG J L, LIU D. Passive localization of mixed near-field and far-field sources using two-stage MUSIC algorithm. IEEE Trans. on Signal Processing, 2009, 58(1): 108–120.
[17] HE J, LI L N, SHU T. Localization of near-field sources for exact source-sensor spatial geometry. IEEE Signal Processing Letters, 2020, 27: 1040–1044.
[18] HSU Y S, WONG K T, YEH L. Mismatch of near-field bearing-range spatial geometry in source-localization by a uniform linear array. IEEE Trans. on Antennas and Propagation, 2011, 59(10): 3658–3667.
[19] HE J, LI L N, SHU T. Bearing and range estimation with an exact source-sensor spatial model. IET Signal Processing, 2020, 14(9): 614–623.
[20] HUANG Y D, BARKAT M. Near-field multiple source localization by passive sensor array. IEEE Trans. on Antennas and Propagation, 1991, 39(7): 968–975.
[21] WEISS A J, FRIEDLANDER B. Range and bearing estimation using polynomial rooting. IEEE Journal of Oceanic Engineering, 1993, 18(2): 130–137.
[22] SINGH P R, WANG Y D, CHARGE P. An exact model-based method for near-field sources localization with bistatic MIMO system. Sensors, 2017, 17(4): 723.
[23] SINGH P R, WANG Y D, CHARGE P. A correction method for the near field approximated model based localization techniques. Digital Signal Processing, 2017, 67: 76–80.
[24] RAO B D, HARI K V S. Performance analysis of root-MUSIC. IEEE Trans. on Acoustics, Speech, and Signal Processing, 1989, 37(12): 1939–1949.
[25] LI J Z, WANG Y D, GANG W. Signal reconstruction for near-field source localisation. IET Signal Processing, 2015, 9(3): 201–205.
[26] LI J Z, WANG Y D, LE BASTARD C, et al. Simplified high-order DOA and range estimation with linear antenna array. IEEE Communications Letters, 2016, 21(1): 76–79.
[27] HORN R A, JOHNSON C R. Matrix analysis. Cambridge: Cambridge University Press, 2012.
[28] CHARGE P, WANG Y D, SAILLARD J. A non-circular sources direction finding method using polynomial rooting. Signal Processing, 2001, 81(8): 1765–1770.
[29] PETERSEN K B, PEDERSEN M S. The matrix cookbook vol.7. Denmark: Technical University of Denmark, 2008.
[30] BEGRICHE Y, THAMERI M, ABED-MERAIM K. Exact conditional and unconditional Cramer-Rao bounds for near field localization. Digital Signal Processing, 2014, 31: 45–58.

Biographies

PAN Jingjing was born in 1991. She received her B.S. and M.S. degrees in cartography and geographic information science from East China Normal University and Beijing Normal University, in 2012 and 2015, respectively. In 2019, she received her Ph.D. degree in electronic systems and radar signal processing from Polytech Nantes, University of Nantes, France. She is now a post-doctoral fellow in Department of Electronic Engineering, Nanjing University of Aeronautics and Astronautics, Nanjing, China. Her research interests include array signal processing and nondestructive testing.
E-mail: jingjingpan@nuaa.edu.cn

SINGH Parth Raj was born in 1989. He received his M.S. and Ph.D. degrees in electronic systems and radar signal processing from Polytech Nantes, University of Nantes, in 2014 and 2017, respectively. He is currently an engineer at International Electronics Engineering S.A., Bissen, Luxembourg. His research interests include array signal processing and vital sign monitoring systems.
E-mail: parth-raj.singh@iee.lu

MEN Shaoyang was born in 1988. He received his M.S. degree in electronic systems and radar signal processing from Polytech Nantes, University of Nantes, France, in 2013, and M.S. degree in communication and information system from South China University of Technology, Guangzhou, China, in 2014. In 2016, he received his Ph.D. degree in digital communications systems from Polytech Nantes, University of Nantes, France. He has been an assistant professor with Guangzhou University of Chinese Medicine, China, since 2017. His current research interests include array signal processing, cognitive wireless sensor networks, and medical image processing.
E-mail: shaoyang.men@gzucm.edu.cn